

## Accepted Manuscript

SAR optimization studies on modified salicylamides as a potential treatment for acute myeloid leukemia through inhibition of the CREB pathway

Hee-Don Chae, Nick Cox, Samanta Capolicchio, Jae Wook Lee, Naoki Horikoshi, Sharon Kam, Andrew Ng, Jeffrey Edwards, Tae-León Butler, Justin Chan, Yvonne Lee, Garrett Potter, Mark C. Capece, Corey W. Liu, Soichi Wakatsuki, Mark Smith, Kathleen M. Sakamoto

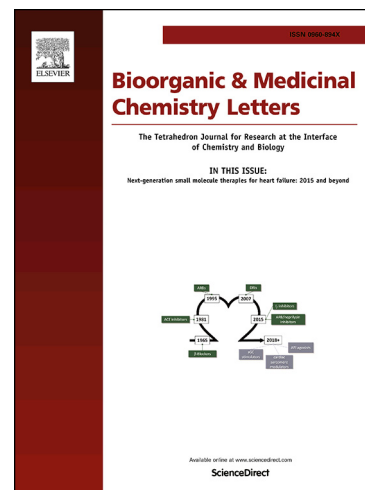
PII: S0960-894X(19)30403-2  
DOI: <https://doi.org/10.1016/j.bmcl.2019.06.023>  
Reference: BMCL 26501

To appear in: *Bioorganic & Medicinal Chemistry Letters*

Received Date: 23 April 2019  
Revised Date: 12 June 2019  
Accepted Date: 17 June 2019

Please cite this article as: Chae, H-D., Cox, N., Capolicchio, S., Wook Lee, J., Horikoshi, N., Kam, S., Ng, A., Edwards, J., Butler, T-L., Chan, J., Lee, Y., Potter, G., Capece, M.C., Liu, C.W., Wakatsuki, S., Smith, M., Sakamoto, K.M., SAR optimization studies on modified salicylamides as a potential treatment for acute myeloid leukemia through inhibition of the CREB pathway, *Bioorganic & Medicinal Chemistry Letters* (2019), doi: <https://doi.org/10.1016/j.bmcl.2019.06.023>

This is a PDF file of an unedited manuscript that has been accepted for publication. As a service to our customers we are providing this early version of the manuscript. The manuscript will undergo copyediting, typesetting, and review of the resulting proof before it is published in its final form. Please note that during the production process errors may be discovered which could affect the content, and all legal disclaimers that apply to the journal pertain.



SAR optimization studies on modified salicylamides as a potential treatment for acute myeloid leukemia through inhibition of the CREB pathway

Hee-Don Chae<sup>a</sup>, Nick Cox<sup>b</sup>, Samanta Capolicchio<sup>b</sup>, Jae Wook Lee<sup>a</sup>, Naoki Horikoshi<sup>c,d</sup>, Sharon Kam<sup>a</sup>, Andrew Ng<sup>b</sup>, Jeffrey Edwards<sup>a</sup>, Tae-León Butler<sup>a</sup>, Justin Chan<sup>a</sup>, Yvonne Lee<sup>a</sup>, Garrett Potter<sup>b</sup>, Mark C. Capece<sup>e</sup>, Corey W. Liu<sup>f</sup>, Soichi Wakatsuki<sup>c,g</sup>, Mark Smith<sup>b\*</sup>, Kathleen M. Sakamoto<sup>a\*</sup>

<sup>a</sup>Department of Pediatrics, Stanford University School of Medicine, Stanford, CA, USA

<sup>b</sup>Medicinal Chemistry Knowledge Center, Stanford ChEM-H, Stanford, CA, USA

<sup>c</sup>Department of Structural Biology, Stanford University School of Medicine, Stanford, CA, USA

<sup>d</sup>Life Science Center for Survival Dynamics, Tsukuba Advanced Research Alliance (TARA), University of Tsukuba, 1-1-1 Tennodai, Tsukuba, Ibaraki 305-8575, Japan

<sup>e</sup>Department of Chemistry, Stanford University, Stanford, CA, USA

<sup>f</sup>Macromolecular Structure Knowledge Center, Stanford ChEM-H, Stanford, CA, USA

<sup>g</sup>BioSciences Division, SLAC National Accelerator Laboratory, Menlo Park, CA, USA

**\*Correspondence to:**

Kathleen M. Sakamoto, M.D., Ph.D.

Division of Hematology/Oncology

Department of Pediatrics

Stanford University

269 Campus Drive, CCSR 1215C

Stanford, California 94305-5162

[kmsakamo@stanford.edu](mailto:kmsakamo@stanford.edu)

Telephone: 650-725-7126

Fax: 650-723-6700

Mark Smith, Ph.D.

Medicinal Chemistry Knowledge Center

Stanford ChEM-H

Stanford University

CCSR 3110

269 Campus Drive,

Stanford, CA 94304

[mxsmith@stanford.edu](mailto:mxsmith@stanford.edu)

Telephone: 415-706-4498

Keywords: Salicylamide, Acute Myeloid Leukemia, small molecule, CREB, CBP

**Abstract**

Disruption of cyclic adenosine monophosphate response element binding protein (CREB) provides a potential new strategy to address acute leukemia, a disease associated with poor prognosis, and for which conventional treatment options often carry a significant risk of morbidity and mortality. We describe the structure-activity relationships (SAR) for a series of XX-650-23 derived from naphthol AS-E phosphate that disrupts binding and activation of CREB by the CREB-binding protein (CBP). Through the development of this series, we identified several salicylamides that are potent inhibitors of acute leukemia cell viability through inhibition of CREB-CBP interaction. Among them, a biphenyl salicylamide, compound **71**, was identified as a potent inhibitor of CREB-CBP interaction with improved physicochemical properties relative to previously described derivatives of naphthol AS-E phosphate.

Acute leukemia is a rapidly progressing hematological malignancy that begins in either lymphoid (acute lymphoblastic leukemia (ALL)) or myeloid (acute myeloid leukemia (AML)) cells. Acute leukemias are characterized by the rapid clonal accumulation of immature lymphoid or myeloid progenitors from the accumulation of several oncogenic mutations with resultant multilineage cytopenia.<sup>1, 2</sup> AML is the most common cause of leukemia death, while ALL is the most common type of cancer in childhood.<sup>3, 4</sup> Even with intensive chemotherapy and hematopoietic stem cell transplantation, the overall 5-year survival for AML is less than 50% in younger patients and less than 10% in patients over 65-years old, and for ALL is less than 80% in younger patients and less than 20% in patients over 65-years old.<sup>5</sup> In addition, treatment of acute leukemia is associated with a variety of long-term complications and a high risk of mortality.<sup>6-8</sup> Therefore, the discovery of novel therapies that are more effective and less toxic would be of great clinical benefit.

Transcription factors control the expression of essential genes to maintain normal hematopoiesis. Mutations or dysregulated expression of these transcription factors play important roles in leukemogenesis.<sup>9</sup> Transcription factors have been considered as difficult drug targets, however, recent studies have shown that transcription factors can be targeted for cancer therapy by inhibiting their association with interacting cofactors.<sup>10, 11</sup> We have studied the cAMP response element binding protein (CREB), a transcription factor that promotes AML cell proliferation and survival, as a potential therapeutic target for acute leukemia. Overexpression of CREB protein in AML cells is associated with a significantly worse prognosis.<sup>12, 13</sup> CREB overexpression in AML cells augments their growth rate and confers resistance to apoptosis.<sup>12</sup> Conversely, CREB knockdown in AML cells decreases cell proliferation and induces apoptosis without any effects on long-term engraftment of hematopoietic stem cells (HSCs).<sup>14, 15</sup> Upon activation by phosphorylation at Ser133 of the Kinase Inducible Domain (KID), CREB recruits co-activator CREB binding protein (CBP) through the interaction of phosphorylated KID with the KID Interacting (KIX) domain. The CREB/CBP complex turns on the expression of CREB-driven genes that regulate cell proliferation and survival.<sup>16-18</sup>

Using an NMR-based screening approach to identify small molecules that bind to KIX, Montminy *et al.* reported that KG-501 **1** disrupted CREB-CBP interaction with an IC<sub>50</sub> of around 90 μM, but attenuated the transcriptional activity of CREB when added to cells with a much higher potency (Figure 1).<sup>19</sup> Subsequent work by Xiao and coworkers showed that KG-501 **1** is neither stable in tissue culture media nor cell permeable and that the dephosphorylated product, naphthol AS-E **2**, is significantly more potent in cells, presumably due to improved permeability (Figure 1).<sup>20</sup> Subsequent structure-activity relationship (SAR) studies of **2** by Xiao showed that a small, electron-withdrawing group at the para position in the phenyl ring was favored for inhibiting KIX-KID interaction and cancer cell viability through the downregulation of CREB-dependent gene expression.<sup>21</sup> To demonstrate the feasibility of targeting CREB as a treatment for acute leukemia, we recently described a small molecule inhibitor of CREB, XX-650-23 (*N*-(4-cyanophenyl)-3-hydroxy-2-naphthamide) **3**, a compound originally based on **2** in collaboration with Xiao's group.<sup>22</sup> Compound **3** changes the expression of CREB-target genes, leading to cell-cycle arrest and apoptosis of AML cells and increased survival of AML xenograft mice with no toxicity to normal cells or animals. Despite significant interest in the development of clinical candidates based on **3**, little is known about the SAR for this scaffold. In this work, we highlight our recent efforts to develop a comprehensive understanding of SAR for **3** with the goal of identifying a lead candidate for acute leukemia therapy with improved potency and physicochemical properties.

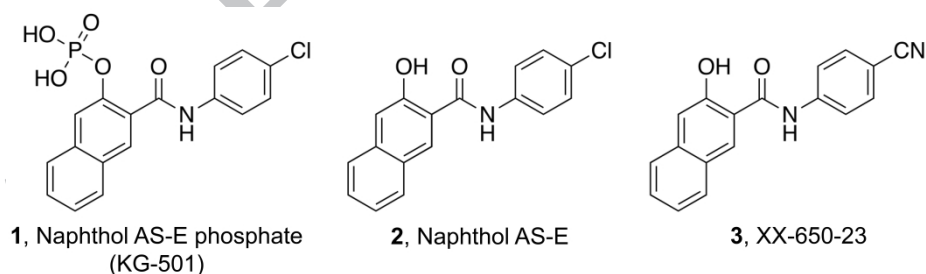


**Figure 1.** Structures of the CREB-CBP binding inhibitor KG-501 (**1**) and CREB-CBP pathway inhibitors naphthol AS-E (**2**) and XX-650-23 (**3**).

Compound **3** binds specifically to the CREB KIX domain and was found to suppress the proliferation of AML cell lines and primary human AML cells with low micromolar  $IC_{50}$ . **3** inhibits histone H3 K27 acetylation in CREB-bound genes and CREB KIX-CBP KID domain interaction, resulting in suppression of CREB-dependent transcriptional activity to induce apoptosis and G1/S arrest in AML cells. Furthermore, **3** prolonged the median survival and reduced disease burden in AML xenograft mice.<sup>22</sup> However, due to its moderate potency and relatively poor pharmacokinetic properties, **3** is not suitable for clinical application. In order to develop a more potent and metabolically stable CREB-CBP inhibitor, we decided to develop a better understanding of the effect of each structural element on the potency and metabolic stability of **3** following a strategy outlined in **Figure 2**. Using this approach, we planned to explore the SAR of various salicylamides in four key areas: (a) the evaluation of naphthyl mimetics, (b) substitutes for the inter-connecting amide group, and (c) the effect of different substituents and substitution patterns on the salicyl and anilide ring systems. The inhibitory potency of these compounds was then assessed on cellular viability of acute leukemia cell lines and KIX-KID interaction. Potent lead compounds were further investigated for the CREB KIX-CBP KIX domain interaction inhibition potency, *in vitro* toxicity in normal bone marrow cells and metabolic stability.

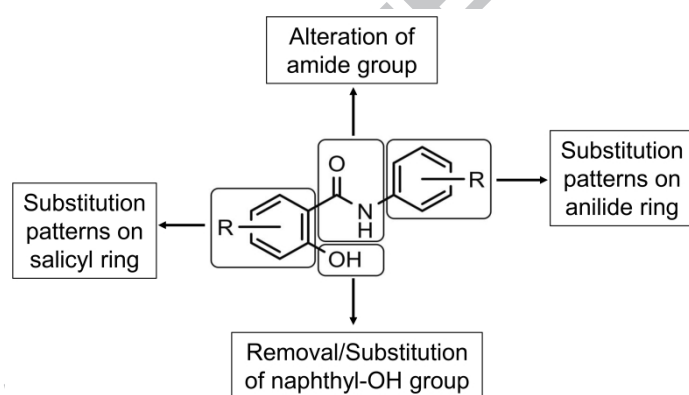


**Figure 2.** Strategy to probe structure-activity relationships (SAR) of XX-650-23 (**3**).

Our initial efforts focused on the role of the naphthalen-2-ol group of **3**. As shown in **Table 1**, removal (**4**) or methylation (**5**) of the naphthyl-OH group completely abolished the cytotoxic activity

against AML cell lines, HL-60 and KG-1. Interestingly, the acetylated derivative, **6**, showed similar potency in inhibiting the viability of AML cell lines. It is possible that this ester is hydrolyzed to release compound **1** *in vitro*, which could explain the similar IC<sub>50</sub> values in both AML cell lines tested. It is worth noting that this could allow for the exploration of a pro-drug strategy in order to modulate the physicochemical properties of **3**. In an effort to explore other hydrogen-bond donors, anilines (**7** and **8**), indole (**9**) and 2-pyridone (**10**) analogs were tested but all were observed to have little biological activity against AML cells. This suggests that the presence of the naphthalen-2-ol is essential for the biological activity of **3**.

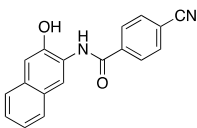
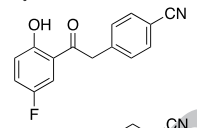
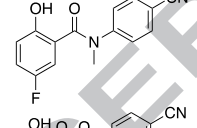
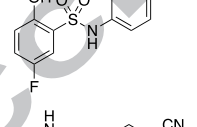
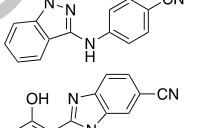
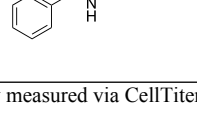
**Table 1.** SAR of naphthalen-2-ol modifications.

Entry	R =	Cell IC <sub>50</sub> (μM) <sup>a</sup>	
		HL-60	KG-1
	$\text{R}-\text{C}(=\text{O})\text{OH} \xrightarrow[\text{DCM, 25 }^\circ\text{C, 12 h}]{\text{1. SOCl}_2 (5.0 \text{ equiv}), \text{DMF} (0.2 \text{ equiv})} \text{R}-\text{C}(=\text{O})\text{NH}-\text{C}_6\text{H}_4-\text{CN}$ $\xrightarrow[\text{DCM, 25 }^\circ\text{C, 12 h}]{\text{2. 4-aminobenzonitrile (2 equiv)}} \text{R}-\text{C}(=\text{O})\text{NH}-\text{C}_6\text{H}_3(\text{OH})-\text{CN}$		
<b>3</b>		1.58	1.23
<b>4</b>		> 10	> 10
<b>5</b>		> 10	> 10
<b>6</b>		1.69	1.70
<b>7</b>		> 10	> 10
<b>8</b>		>10	> 10
<b>9</b>		> 10	> 10
<b>10</b>		>10	> 10

<sup>a</sup>Cell viability measured via CellTiter-Glo kit; average of triplicates reported.

To determine the importance of the inter-connecting amide moiety, we first explored the constitutional isomer of **3** in which the carbonyl and amide nitrogen are transposed (**11**), and found it to be inactive against AML cells. Substitution with a ketone (**12**) or *N*-methylation (**13**) also displayed no activity in AML cells, suggesting that the amide hydrogen plays a key role as a H-bond donor or perhaps stabilizes the desired conformation. Similarly, replacement of the amide group with a sulfonamide **14** abolished activity. The salicylamide isosteres, **15** and **16**, were also prepared and tested. The substitution of salicylanilide motif with benzimidazole or aminoindazole groups did not produce active compounds against AML cell lines, suggesting that the salicylanilide group may be uniquely active.

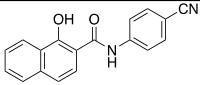
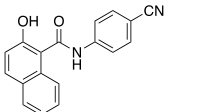
**Table 2.** SAR of amide group modifications.

Entry	Structure	Cell IC <sub>50</sub> (μM) <sup>a</sup>	
		HL-60	KG-1
11		> 10	> 10
12		> 10	> 10
13		> 10	> 10
14		> 10	> 10
15		> 10	> 10
16		> 10	> 10

<sup>a</sup>Cell viability measured via CellTiter-Glo kit; average of triplicates reported.

Previous exploration of SAR for this motif focused on substitutions of the anilide ring while much less was known about SAR of the salicyl portion of **3**. We prepared the 1-hydroxyl-2-naphthamide **17** and 2-hydroxy-1-naphthamide **18** analogs (**Table 3**). These modifications slightly decreased the potency in both AML cell lines, suggesting that substituents in positions 4 and 5 of the salicyl ring are preferred.

**Table 3.** Antiproliferative effects of naphthamide analogs on AML cells.

Entry	Structure	Cell IC <sub>50</sub> (μM) <sup>a</sup>	
		HL-60	KG-1
<b>17</b>		3.41	2.72
<b>18</b>		4.43	3.76

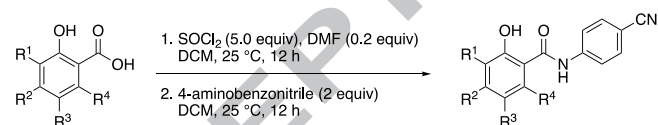
<sup>a</sup>Cell viability measured via CellTiter-Glo kit; average of triplicates reported.

We further explored the effect of substituents in the salicyl ring. The synthetic scheme for preparing a series focusing on the salicyl ring is depicted at the top of **Table 4**: generally, salicylic acid derivatives were first converted to the corresponding acid chlorides using SOCl<sub>2</sub>, which was followed by the amide coupling step using excess aniline (See **Supplemental Information** for experimental details). Replacing the fused naphthyl ring with a biaryl system resulted in a slight gain of potency when a phenyl group occupied position 4 (**19**), but a slight loss of potency with the phenyl group in position 5 (**20**). Replacement of the phenyl ring with 4-pyridyl (**21** and **22**) and 3-pyridyl (**23** and **24**) rings led to a 5- to 10-fold drop in potency. Given these results, our next efforts were focused on understanding the SAR of salicylamides containing a phenyl (**25**) rather than a naphthyl ring. Removal of substituents on the phenyl ring decreases activity suggesting that functional groups *meta* and *para* to the carbonyl group are necessary for potency (**25**). In general, it was found that the presence of a halogen in position 5 (R<sup>3</sup>) of the salicyl ring, such compounds **29** and **30**, correlated with improved potency relative to the unsubstituted

analog **25**. A moderate increase in potency was observed with a benzyl group **26**, whereas a minor boost in potency was seen with trifluoromethyl **37** and trifluoromethyl **40**. The only significant decrease was seen with the para-methoxy substituent **44**. A similar SAR pattern was observed for substituents at position 4 ( $R^2$ ) and very little, if any, improvement could be made with substitution at positions 3 and 6 relative to the *N*-(4-cyanophenyl)salicylamide **25**. The nature of the halogen also plays a role: the fluoro-derivatives were, in all cases, slightly less potent than the bromo- or chloro- analogs. However, it is not clear that this is an electronic effect or simply related to slight differences in lipophilicity affecting cell permeability.

Next, we explored the effect of combined substituents on the salicyl ring in order to understand whether double substitutions have a synergistic effect or lead to a loss of potency (**46** and **47**). We observed the highest potency when a phenyl group occupied position 4 (**19**), or the introduction of bromine (**29**) or chlorine (**30**) at position 5 of the salicyl ring. Compounds that contained both a phenyl group at position 5 and a halogen (**46** and **47**) at position 4 showed no further significant improvement in potency.

**Table 4.** SAR of 2-Hydroxy-phenyl modifications.



Entry	$R^1$	$R^2$	$R^3$	$R^4$	Cell IC <sub>50</sub> ( $\mu\text{M}$ ) <sup>a</sup>	
					HL-60	KG-1
<b>19</b>	H	Ph	H	H	0.70	0.41
<b>20</b>	H	H	Ph	H	1.35	1.30
<b>21</b>	H	4-Pyridyl	H	H	7.09	8.84
<b>22</b>	H	H	4-Pyridyl	H	5.41	7.99
<b>23</b>	H	3-Pyridyl	H	H	6.66	7.94
<b>24</b>	H	H	3-Pyridyl	H	7.96	8.33
<b>25</b>	H	H	H	H	4.62	5.37
<b>26</b>	H	H	Bn	H	1.74	1.93
<b>27</b>	Br	H	H	H	2.91	3.26
<b>28</b>	F	H	H	H	5.39	9.69

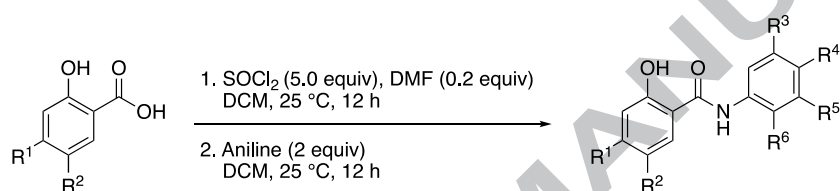
29	H	H	Br	H	0.62	1.29
30	H	H	Cl	H	0.70	1.86
31	H	F	H	H	1.38	3.15
32	H	H	F	H	1.42	2.67
33	H	Br	H	H	1.21	1.45
34	H	Cl	H	H	1.30	1.92
35	H	H	H	F	> 10	> 10
36	H	CF <sub>3</sub>	H	H	1.03	1.44
37	H	H	CF <sub>3</sub>	H	3.12	4.81
38	Me	H	H	H	> 10	8.98
39	H	Me	H	H	2.42	2.56
40	H	H	Me	H	3.92	3.37
41	H	H	H	Me	6.86	7.94
42	MeO	H	H	H	> 10	> 10
43	H	MeO	H	H	5.47	5.43
44	H	H	MeO	H	> 10	> 10
45	H	H	H	MeO	> 10	> 10
46	H	Ph	Cl	H	0.52	0.48
47	H	Ph	Br	H	0.70	0.85

<sup>a</sup>Cell viability measured via CellTiter-Glo kit; average of triplicates reported.

Concurrent with an exploration of SAR of the salicyl ring, a series focusing on the anilide moiety was generated. As derivatives with halogens in either position 4 or 5 or a non-substituted phenyl in position 4 of the salicyl ring were the most potent against AML cell lines (**Table 4**), we designed several salicylamide derivatives bearing different substituents on the anilide ring and explored their activity against leukemia cell lines (**Table 5**). Derivatives with a cyano group in position 4 (**48**) or without a cyano group in the position 2 (**49**) were significantly less potent than compounds with the same group in position 4 of the anilide group (**32**). In general, it was found that anilides bearing electron-withdrawing groups were significantly more potent. When trifluoromethyl, trifluoromethoxy, and nitro groups occupied the position 3 (R<sup>4</sup>) or 4 (R<sup>5</sup>) of the anilide ring, we observed increased potency in AML and ALL cell lines (Table 5 entries **50–63**), while derivatives containing fluoro, chloro, acetyl, ester, phenyl, methoxy, and sulfonyl groups were significantly less potent (data not shown). Based on our observations that the most potent compounds contained anilides bearing electron withdrawing groups, several analogs containing two substituents on the anilide ring were prepared. We observed that compounds with two

trifluoromethyl groups (**Table 5**, entries **64–73**) were, in general, more potent in AML and ALL cell lines than compounds with single trifluoromethyl group on the anilide ring. While single halogen substituents on the anilide ring decreased potency, we observed a boost in potency when two halogens were introduced (**74–78**). The combination of a chloro group with either a trifluoromethoxy or a trifluoromethyl substituent did not further enhance the potency against leukemic cells (**79–84**). Similarly, derivatives with both a chloro and a cyano group did not significantly increase the potency compared to derivatives bearing two chloride groups (**85–87**).

**Table 5.** SAR for anilide ring.



#	R <sup>1</sup>	R <sup>2</sup>	R <sup>3</sup>	R <sup>4</sup>	R <sup>5</sup>	R <sup>6</sup>	Cell IC <sub>50</sub> (μM) <sup>a</sup>			
							HL-60	KG-1	Jurkat	Nalm6
48	H	F	CN	H	H	H	7.75	9.10	n.d. <sup>b</sup>	n.d.
49	H	F	H	H	H	H	> 10	> 10	n.d.	n.d.
50	H	F	H	CF <sub>3</sub>	H	H	0.49	1.70	0.58	2.09
51	F	H	H	CF <sub>3</sub>	H	H	0.68	0.74	0.80	1.53
52	H	F	H	H	CF <sub>3</sub>	H	0.97	1.01	0.84	1.80
53	H	Cl	H	CF <sub>3</sub>	H	H	0.51	0.74	0.71	1.21
54	Cl	H	H	CF <sub>3</sub>	H	H	0.63	0.58	0.67	1.18
55	H	Br	H	CF <sub>3</sub>	H	H	0.58	0.61	0.62	1.09
56	Br	H	H	CF <sub>3</sub>	H	H	0.36	0.34	0.50	0.69
57	CF <sub>3</sub>	H	H	CF <sub>3</sub>	H	H	0.38	0.78	0.82	1.12
58	Ph	Cl	H	CF <sub>3</sub>	H	H	0.49	0.77	1.16	0.80
59	Ph	Br	H	CF <sub>3</sub>	H	H	0.54	0.40	0.74	1.00
60	F	Br	H	CF <sub>3</sub>	H	H	0.45	0.82	0.88	1.30
61	H	F	H	OCF <sub>3</sub>	H	H	0.85	0.78	0.81	1.21
62	H	F	H	H	OCF <sub>3</sub>	H	0.73	0.83	0.70	1.37
63	H	F	H	NO <sub>2</sub>	H	H	0.52	1.10	0.94	2.08
64	H	F	CF <sub>3</sub>	H	CF <sub>3</sub>	H	0.32	0.47	0.50	0.62
65	H	Cl	CF <sub>3</sub>	H	CF <sub>3</sub>	H	0.16	0.50	0.48	0.63
66	Cl	H	CF <sub>3</sub>	H	CF <sub>3</sub>	H	0.20	0.62	0.57	0.85
67	H	Br	CF <sub>3</sub>	H	CF <sub>3</sub>	H	0.29	0.30	0.35	0.59
68	Br	H	CF <sub>3</sub>	H	CF <sub>3</sub>	H	0.27	0.83	0.93	1.20
69	Ph	H	CF <sub>3</sub>	H	CF <sub>3</sub>	H	1.14	0.86	1.24	1.58
70	Ph	Cl	CF <sub>3</sub>	H	CF <sub>3</sub>	H	0.79	0.43	0.54	0.56
71	Ph	Br	CF <sub>3</sub>	H	CF <sub>3</sub>	H	0.43	0.30	0.68	0.84
72	F	Cl	CF <sub>3</sub>	H	CF <sub>3</sub>	H	0.43	0.47	0.73	2.13
73	F	Br	CF <sub>3</sub>	H	CF <sub>3</sub>	H	0.25	0.51	0.70	0.95
74	H	F	Cl	H	Cl	H	0.60	0.78	0.71	1.44
75	H	F	H	Cl	H	Cl	0.89	0.85	0.88	1.62

76	H	F	Cl	Cl	H	H	0.66	0.76	0.67	1.37
77	H	F	Cl	Br	H	H	0.60	0.67	0.86	1.25
78	H	Cl	Br	Cl	H	H	0.78	0.68	1.35	3.07
79	H	Cl	Cl	OCF <sub>3</sub>	H	H	0.45	0.46	0.84	1.05
80	H	F	Cl	OCF <sub>3</sub>	H	H	0.55	0.37	0.70	1.00
81	H	Cl	H	OCF <sub>3</sub>	H	Cl	0.65	0.62	0.88	1.35
82	CF <sub>3</sub>	H	Cl	OCF <sub>3</sub>	H	H	0.38	0.64	0.79	0.95
83	H	Cl	Cl	CF <sub>3</sub>	H	H	0.46	0.45	0.69	1.22
84	H	F	CF <sub>3</sub>	Cl	H	H	0.60	0.54	0.53	0.97
85	Br	H	Cl	CN	H	H	0.44	0.96	0.75	0.92
86	H	Cl	H	CN	H	Cl	0.50	0.86	0.62	0.73
87	Br	H	H	CN	H	Cl	0.73	0.79	0.75	1.86
88	H	F	H	NO <sub>2</sub>	H	Cl	0.28	0.49	0.53	0.91
89	H	Cl	H	NO <sub>2</sub>	H	Cl	0.30	0.36	0.40	0.62

<sup>a</sup>Cell viability measured via CellTiter-Glo kit; average of triplicates reported.

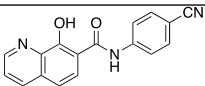
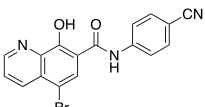
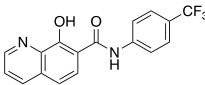
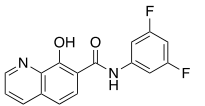
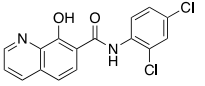
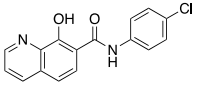
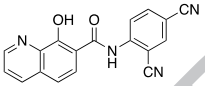
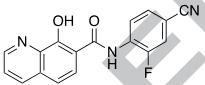
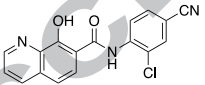
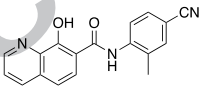
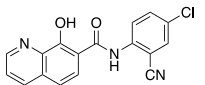
<sup>b</sup>n.d.: not determined.

We found compound **88** to be particularly intriguing, as it bears significant resemblance to the widely-used anthelmintic Niclosamide **89**,<sup>23-25</sup> having the salicylanilide core, an electron withdrawing halogen para to the naphthyl hydroxyl group of the salicyl ring, and an electron-withdrawing nitro group para to the anilide. Niclosamide has been reported to have anti-tumor activity in several cancers by targeting several oncogenic signaling pathways including Wnt/ $\beta$ -catenin, mTORC1, STAT3, NF- $\kappa$ B, and Notch.<sup>25-30</sup> Indeed, when Niclosamide was tested in our hands, it was found to inhibit cellular viability of AML cells by inducing apoptosis and cell cycle arrest, with minimal toxicity in normal bone marrow cells.<sup>31</sup> Additionally, Niclosamide was observed to inhibit KIX- KID binding interaction and CREB-dependent transcription in a dose-dependent manner. Primary xenograft models with AML patient samples demonstrated that Niclosamide inhibits AML disease progression *in vivo* and prolongs survival. Niclosamide also potentiates the cytotoxic effect of other chemotherapy drugs including Daunorubicin, Vincristine, and Mitoxantrone.<sup>31</sup>

Finally, we decided to investigate the potency of 8-hydroxyquinolines derivatives. Replacement of the naphthyl ring with an 8-hydroxyquinoline derivative (**90**) displayed impressive potency against AML and ALL cell lines except KG1. We further investigated the activity of derivatives of **90** against leukemia cell lines (**Table 6**). Interestingly, these derivatives with structural modification of the anilide

moiety slightly decreased the potency of all tested derivatives (**92–100**), while the introduction of bromine in the quinoline moiety resulted in similar potency (**91**).

**Table 6.** 8-Hydroxyquinoline modifications.

#	Structure	Cell IC <sub>50</sub> (μM) <sup>a</sup>			
		HL-60	KG-1	Jurkat	Nalm6
<b>90</b>		0.37	2.32	0.18	0.13
<b>91</b>		0.33	n.d. <sup>b</sup>	0.23	0.21
<b>92</b>		0.68	3.51	0.55	0.38
<b>93</b>		0.51	3.34	0.43	0.31
<b>94</b>		0.61	3.56	0.43	0.45
<b>95</b>		0.63	3.30	0.51	0.38
<b>96</b>		0.89	3.77	0.27	0.35
<b>97</b>		0.73	3.26	0.42	0.37
<b>98</b>		0.91	3.67	0.55	0.42
<b>99</b>		0.71	3.24	0.27	0.23
<b>100</b>		0.79	3.54	0.17	0.28

<sup>a</sup>Cell viability measured via CellTiter-Glo kit; average of triplicates reported.

<sup>b</sup>n.d.: not determined.

To confirm whether our lead compounds can inhibit the CREB-CBP pathway, we performed the split Renilla luciferase (RLuc) complementation assay in which the RLuc activity can be reconstituted only when N-terminal RLuc (RLucN) fused with KID and C-terminal RLuc (RLucC) fused with KIX are brought to a close by KIX-KID interactions.<sup>20</sup> Without interaction between KIX and KID domains, the RLuc fragments cannot exhibit emission of light in the presence of substrate coelenterazine. Therefore, the emitted light from the reconstituted Renilla luciferase represents the binding activity of KIX and KID, allowing us to access the KIX-KID interaction inhibition potency of lead compounds in live cells. There was a positive correlation between KIX-KID interaction inhibitory activity and the potency in leukemia cells. Consistent with their loss of potency in leukemia cells (**Tables 1-4**), removal of naphthyl-OH (**4**), modification in the amide group (**11**) or methoxy substituent in the salicyl ring (**44** and **45**) showed significantly less CBP KIX-CREB KID interaction inhibitory activity (**Figure 3**). As the introduction of a bromo (**29**) or chloro (**30**) in position 5 of the salicyl ring modestly improved potency in AML cell lines, their KIX-KID inhibitory potency was marginally increased (**Figure 3**). The presence of two trifluoromethyl groups in anilide ring of compounds with a halogen in position 5 (**66** and **67**) or a non-substituted phenyl in position 4 with a halogen in position 5 (**71**) of the salicyl ring led to the significant enhanced KIX-KID inhibitory activity (**Figure 3**), consistent with their improved potency in leukemia cells. Furthermore, we have assessed the direct inhibitory effect of lead compounds (**66**, **67** and **71**) on KID-KIX interaction with a fluorescence polarization (FP) assay. The assay measures a BODIPY-labeled phosphorylated KID domain of CREB and KIX domain of CBP using FP to provide the degree of KIX-KID interaction. In the presence of an inhibitor, BODIPY-labeled phosphorylated KID domain could not bind to the KID domain, which decreases the FP as a result of the increase in the mobility of the BODIPY-labeled KID domain. Consistent with the split RLuc complementation assay data, these compounds (**66**, **67** and **71**) led to a decrease in fluorescence polarization (**Supplementary Figure 1**). Compounds **66**, **67** and **71** showed a similar potency in leukemia cells and KIX-KID inhibition with **88** and Niclosamide **89** (**Figure 3**), suggesting our lead compounds are targeting CREB-CBP for anti-leukemic activity similar to Niclosamide **89**.

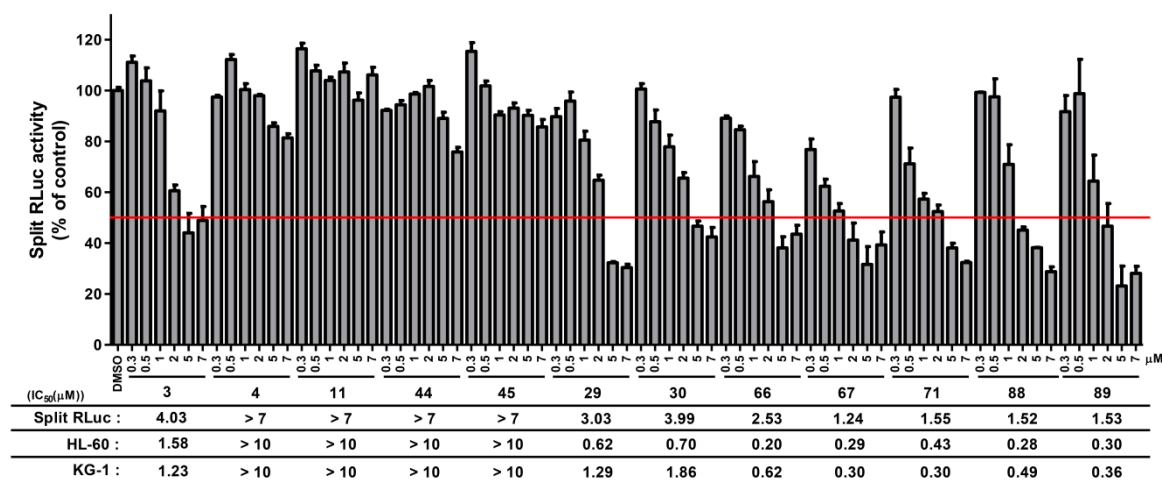


**Figure 3.** Split Renilla luciferase assay for CBP KIX-CREB KID interaction. RLucC-KIX and KID-RLucN expressing vectors were transfected into 293 cells. Transfected cells were treated with compounds half hour before forskolin treatment. Cells were incubated with the indicated amounts of compounds for additional 90 min. If compounds block the association of KIX and KID domain, light emission by Renilla luciferase activity will be diminished. Renilla luciferase activity was measured using coelenterazine. Data are presented as mean  $\pm$  SEM (n=3).

Though their enhanced potency in leukemia cells, 8-hydroxyquinoline derivatives did not inhibit KIX-KID interaction (**Figure 4**), suggesting the naphthyl group is critical to provide specificity for the inhibitory effect on KIX-KID interaction.

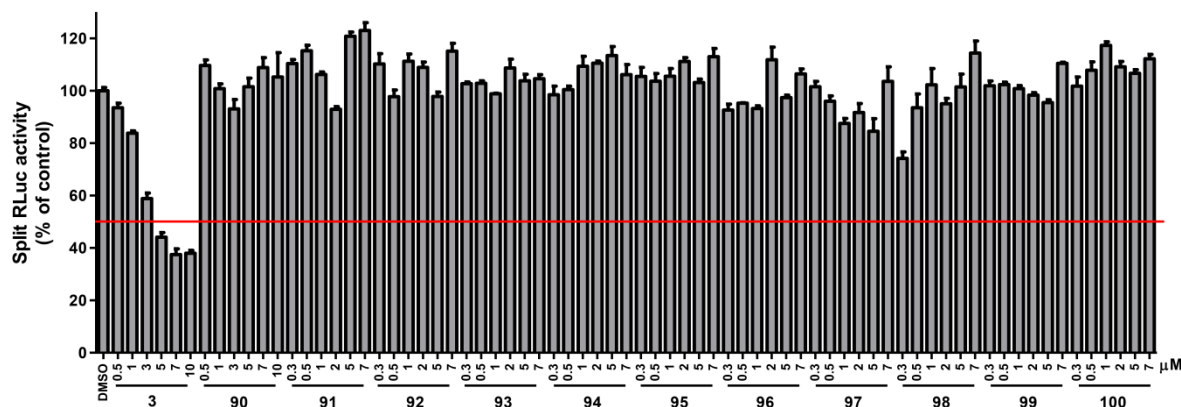


**Figure 4.** Split Renilla luciferase assay for assessing the effects of 8-Hydroxyquinoline derivatives on CBP KIX-CREB KID interaction. HEK 293 cells transfected with RLucC-KIX and KID-RLucN expressing vectors were treated with 8-Hydroxyquinoline derivatives, and then Renilla luciferase activity was measured using coelenterazine. Data are presented as mean  $\pm$  SEM (n=3).

Compound **3** and Niclosamide **89** suppress leukemia cell viability *in vitro* and leukemia disease progression *in vivo* by inhibiting CREB-dependent gene transcription and KIX-KID interaction with little toxicity on normal human hematopoietic cells or mice.<sup>22, 31</sup> As CREB knockdown using shRNA inhibited AML cell growth without affecting the proliferation of normal hematopoietic cells,<sup>14, 15</sup> we expected that targeting CREB would be associated with less toxicity than conventional chemotherapy. Thus, the potential toxicity of lead compounds was assessed in normal bone marrow (BM) progenitor cells. *In vitro* colony formation activity of normal BM hematopoietic progenitor cells was not significantly inhibited up to 10  $\mu$ M of **67** and **71**, consistent with **3** and Niclosamide **89** (Table 7). Though **90** inhibited colony formation activity of normal bone marrow cells ( $IC_{50}$ : 3.07  $\mu$ M), its 10-fold therapeutic window is still enough for clinical application.

Since **66**, **67**, **71**, and **90** showed low toxicity in normal BM cells as well as excellent potency in leukemia cells, these compounds were evaluated for *in vitro* metabolic stability. However, compound **3** and Niclosamide **89** is metabolically unstable, limiting its development as a drug for the treatment of AML.<sup>32</sup> Therefore, we evaluated *in vitro* metabolic stability of our promising lead compounds to

determine what should be further profiled in pharmacokinetic (PK) studies. The microsomal metabolic stabilities of these compounds were determined with human (HLM) and mouse liver microsomes (MLM) (Table 7). **3** and Niclosamide **89** showed poor *in vitro* metabolic stability in both HLM ( $T_{1/2}$ : 44.9 min and 21 min) and MLM ( $T_{1/2}$ : 5.5 min and 6.6 min) (Table 7). **90** showed improved *in vitro* stability in both HLM and MLM ( $T_{1/2}$ : 124.1 min and 156.7 min). Compound **67** showed an excellent potency in leukemia cells and KID-KIX inhibitory activity, however, it was unstable in HLM and MLM assays. *N*-[3,5-Bis(trifluoromethyl)phenyl]-4-chlorosalicylamide **66** observed a significant improvement in stability when incubated with human microsomes ( $T_{1/2}$ : 159 min). However, this modification did not improve metabolic stability in mouse liver microsomes ( $T_{1/2}$ : 31.8 min). Liver microsomes from mouse and human have the specific enzyme activities of cytochrome P450 with different cytochrome P450 isoforms<sup>33</sup>, which can account for the discrepancy we observed for compound **66**. However, compound **71**, bearing a phenyl group in position 4 and bromine at position 5 was stable in both human and mouse liver microsomes.

**Table 7.** Toxicity and *in vitro* metabolic stability data.

#	Structure	Normal BM cells	Metabolic Stability ( $T_{1/2}$ )	
		( $IC_{50}$ ( $\mu$ M))	HLM (min)	MLM (min)
<b>3</b>		> 10	44.9	5.5
<b>67</b>		> 10	52	29.1
<b>71</b>		> 10	159	159
<b>89</b>		> 10	21	6.6



Due to their excellent *in vitro* potency and improved *in vitro* metabolic stability, **71** and **90** were further evaluated by profiling pharmacokinetic (PK) properties in NOD.Cg-Prkdc<sup>scid</sup> Il2rg<sup>tm1Wjl</sup>/SzJ (NSG) mice after single intravenous (IV) administration (2 mg/kg). The time-concentration profiles of Niclosamide **89**, **90**, and **71** in mouse plasma were shown in **Figure 5**, and the pharmacokinetic parameters were listed in **Table 8**. Compared with Niclosamide **89**, **71** displayed a higher plasma concentration (0.12 ng/ml vs. 19.0 ng/ml) and longer elimination phase half-life (0.56 h vs. 2.05 h), suggesting that introduction of a phenyl group in the salicyl ring of **71** led to better pharmacokinetic properties than Niclosamide **89**. Interestingly, compound **90** also showed enhanced pharmacokinetic performance ( $T_{1/2}$ : 2.05 h).

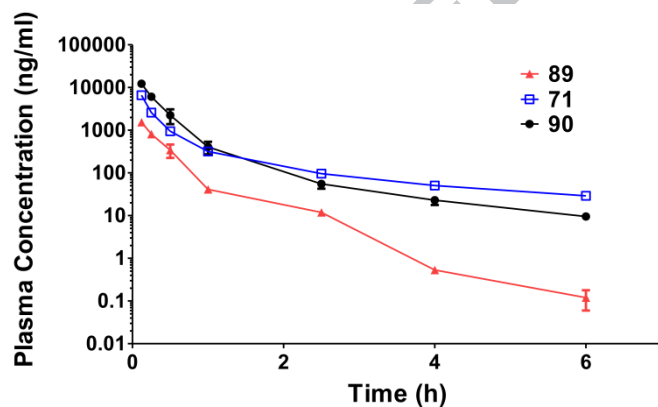


**Figure 5.** The plasma concentrations of **71**, **90**, and Niclosamide **89** after a single intravenous administration to mice. The compounds were dissolved in DMSO/Kolliphor EL (Sigma)/water (3/5/82), and then administered into NOD.Cg-Prkdc<sup>scid</sup> Il2rg<sup>tm1Wjl</sup>/SzJ (NSG) mice intravenously at a dose of 2mg/kg. The levels of compounds were determined in the plasma at various times after the intravenous injection.

**Table 8.** Pharmacokinetic profile of **71**, **90**, and Niclosamide **89**.

#	Dose (mg/kg)	Route	T <sub>1/2</sub> (h)	AUC <sub>0-t</sub> (ng/ml*h)	AUC <sub>0-inf</sub> (ng/ml*h)	MRT <sub>0-inf</sub> (h)	V <sub>z_obs</sub> (mg/(ng/ml))	Cl <sub>obs</sub> ((mg)/(ng/ml)/h)	V <sub>ss_obs</sub> (mg/(ng/ml))
<b>89</b>	2	IV	0.56	536	536	0.404	0.0025	0.0037	0.0015
<b>71</b>	2	IV	2.05	2249	2334	1.016	0.0030	0.00086	0.00087
<b>90</b>	2	IV	1.39	4070	4089	0.458	0.00098	0.00049	0.00022

Compound **1** and Niclosamide **89** induce apoptosis and G1/S arrest.<sup>22, 31</sup> Though **90** showed excellent cellular potency, *in vitro* microsomal stability and PK properties, compound **90** did not inhibit KIX-KID interaction (**Figure 4**). To identify the mechanism of anti-leukemic cell cytotoxicity of **90** and **71**, apoptosis and cell cycle analysis studies of compound-treated cells were performed. Apoptosis was assessed using Annexin-V/DAPI double staining and anti-cleaved PARP (poly(ADP-ribose)polymerase) (cPARP) antibody staining. While both **90** and **71** elicited apoptosis at early (Annexin-V<sup>+</sup>/DAPI<sup>-</sup>) and late (Annexin-V<sup>+</sup>/DAPI<sup>+</sup>) stages after 1 day treatment, significantly fewer cells entered apoptotic stage by compound **90** compared with compound **71** (Annexin-V<sup>+</sup>: 9.3% vs. 39.7%) (**Figure 6A**). We further investigated whether these compounds induced apoptosis through the activation of Caspase-3 by measuring cPARP-positive population<sup>34</sup>. cPARP-positive population was increased 1d after treatment of **90** and **71** (cPARP<sup>+</sup>: 17.3% vs. 58.1%) (**Figure 6B**).

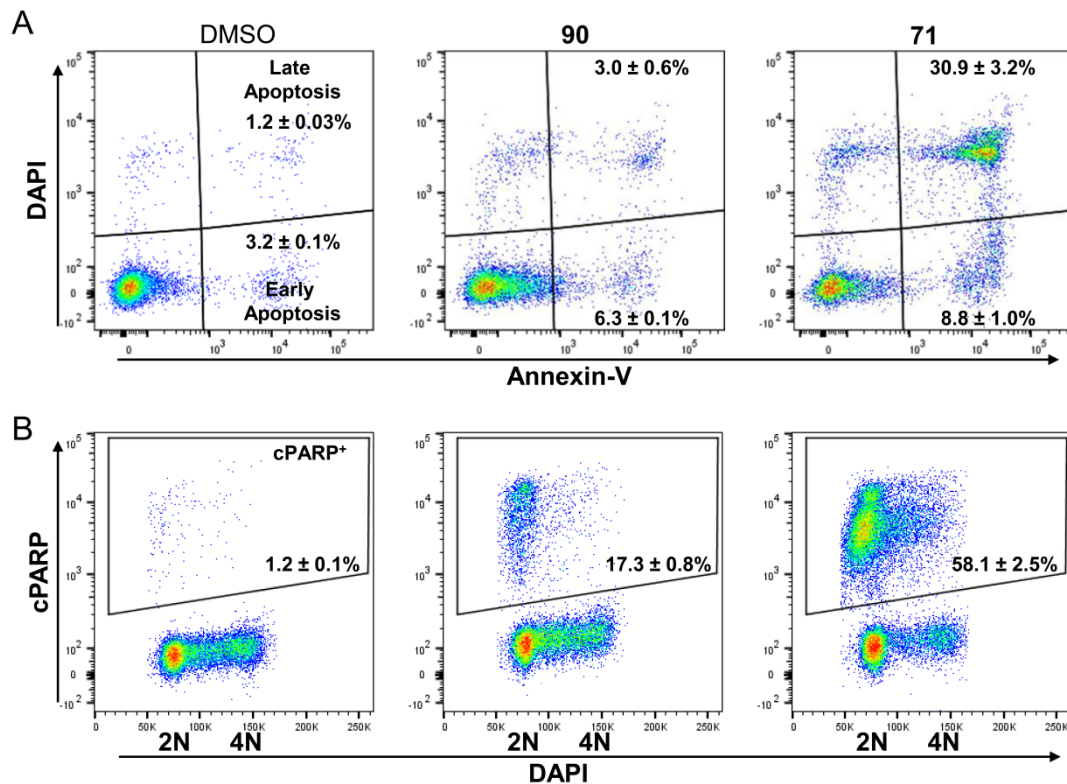


**Figure 6.** Treatment of compound **90** and **71** induces apoptosis. HL60 cells were treated with compounds (1  $\mu$ M) for 1d. (A) Apoptotic cells were assessed by Annexin-V/DAPI double staining. Compound **71** induced a higher percentage of early apoptotic (Annexin-V<sup>+</sup>/DAPI<sup>-</sup>) and late apoptotic (Annexin-V<sup>+</sup>/DAPI<sup>+</sup>) populations than compound **90**. Percentages of early and late apoptotic cells are shown as mean  $\pm$  SEM (n=3). (B) Cells were fixed, and then stained with anti-cleaved PARP (cPARP) antibody and DAPI. Percentages of cPARP<sup>+</sup> apoptotic cells are indicated as mean  $\pm$  SEM (n=3).

Since CREB knockdown using shRNA or CREB inhibition by treatment with compound **3** and Niclosamide causes aberrant cell-cycle progression at the G1/S transition and G1 phase arrest,<sup>22, 31</sup> we further investigated the effects of **90** and **71** on the cell cycle progression. Consistent with **3** and Niclosamide **89** as a CREB pathway inhibitor, **71** induced G1 cell cycle arrest with increased cell population at G1 phase (control vs. **71**-treated cells, 48.37  $\pm$  0.15% vs. 69.77  $\pm$  0.58%, mean  $\pm$  SEM (n = 3), p < .001), but decreased cell populations at S, G2, and M phases (control vs. **71**-treated cells, S: 27.50

$\pm 0.57\%$  vs.  $14.27 \pm 0.15\%$ ; G2:  $21.40 \pm 0.42\%$  vs.  $14.37 \pm 0.43\%$ ; M:  $2.64 \pm 0.06\%$  vs.  $1.23 \pm 0.08\%$ , mean  $\pm$  SEM (n = 3),  $p < .001$ ) (**Figure 7A & B**). Conversely, **90** showed defective S/G2 transition with enhanced percentage of S phase cells (control vs. **90**-treated cells,  $27.50 \pm 0.57\%$  vs.  $33.70 \pm 0.26\%$ , mean  $\pm$  SEM (n = 3),  $p < .001$ , **Figure 7A & B**) and suppressed Cyclin B expression in G2 phase population (Cyclin B MFI, control vs. **90**-treated cells,  $1196.33 \pm 40.48$  vs.  $875.33 \pm 41.90$ , mean  $\pm$  SEM (n = 3),  $p < .01$ , **Figure 7C**). Next, we investigated the effects of **90** and **71** on the expression of CREB target genes, *RFC3* and *POLD2*. *RFC3* and *POLD2*, critical players in DNA synthesis and repair,<sup>35</sup> have been shown to be downregulated by CREB knockdown and CREB inhibitors including Niclosamide **89**.<sup>22, 36, 37</sup> Our quantitative RT-PCR results showed that mRNA expression levels of *RFC3* and *POLD2* are suppressed by compound **71** (Figure 8). This data indicates that **71** exerts its inhibitory effect on leukemia cells by inducing cell cycle arrest at G1 as well as apoptosis through inhibiting CREB-dependent pathway consistent with compound **3** and Niclosamide **89**.

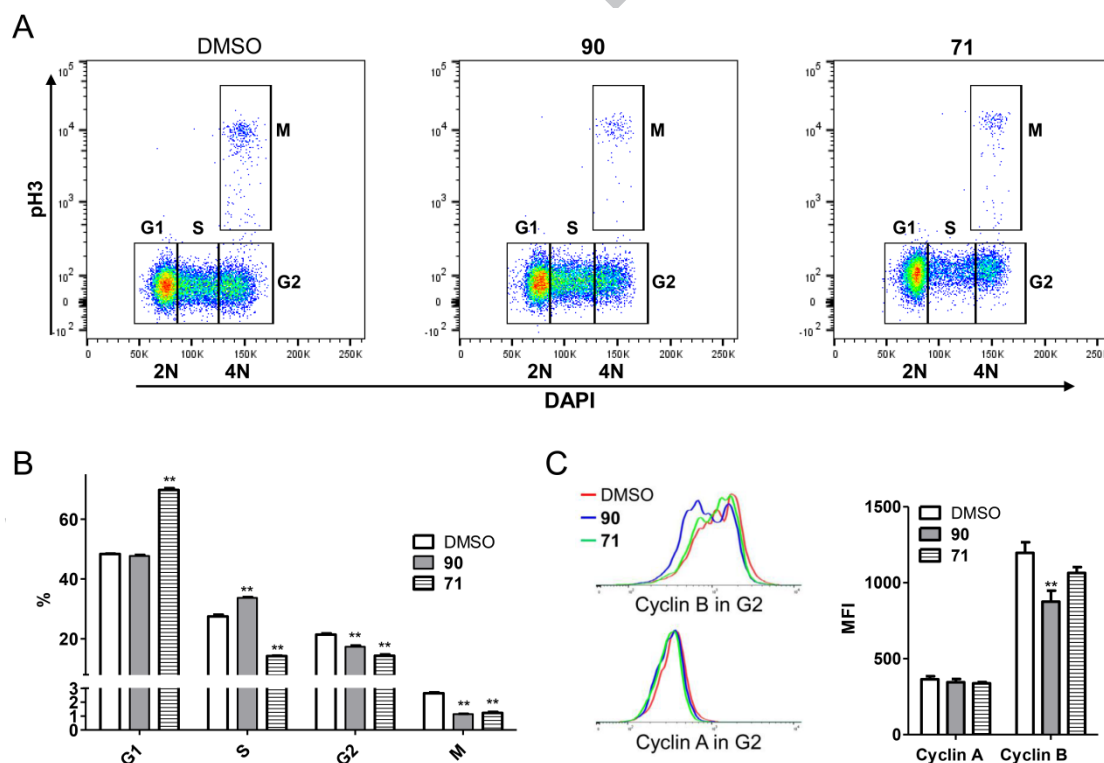


**Figure 7.** Effect of compound **71** and **90** on cell cycle progression. HL60 cells were treated with compounds (1  $\mu$ M) for 1d. Cells were stained for assessing DNA content (DAPI) and levels of p-H3, Cyclin A and Cyclin B. (A) Cell cycle profiles of DMSO or compound-treated HL-60 cells were shown as the bivariate distribution of DNA content versus the level of phosphorylated Histone H3. (B) Percentages of cell populations residing at each cell cycle stage determined by DNA content (DAPI) and levels of p-H3, Cyclin A and Cyclin B using FlowJo software were plotted as mean  $\pm$  SEM (n = 3). (C) Protein levels of the Cyclin A and Cyclin B in G2 phase cells were assessed by flow cytometry analysis. Median Fluorescence Intensities (MFI) of Cyclin A and Cyclin B were graphed as mean  $\pm$  SEM (n = 3). \*\* , p < .01.

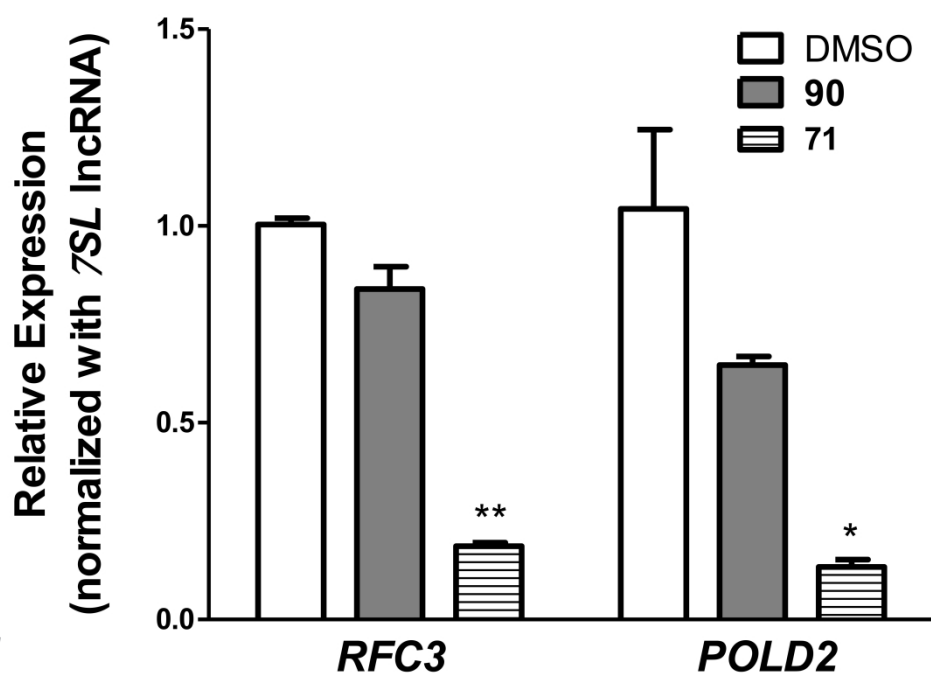


**Figure 8.** Downregulation of CREB-target genes (*RFC3* and *POLD2*) following treatment of compound **71**, not compound **90**. HL60 cells were treated with compound **71** or **90** (1  $\mu$ M) for 1d. *RFC3* and *POLD2* mRNAs were assessed by RT-qPCR and normalized against *7SL* lncRNA expression level. The data represent means of three independent experiments  $\pm$  SEM. \*, p < .05; \*\*, p < .01.

We have conducted a thorough investigation of the SAR around the lead salicylamide, XX-650-23 **3**, and have discovered numerous molecules that have improved potency in acute leukemia cells, CBP KIX-CREB KID interaction inhibitory activity, and physicochemical properties, whilst maintaining low toxicity in normal human hematopoietic cells. Our study showed that adding trifluoromethyl, trifluoromethoxy or nitro group to the position 3 or 4 of the anilide ring significantly increased the potency of XX-650-23 **3** in acute leukemia cells and the inhibitory KIX-KID interaction activity. Furthermore, the addition of a phenyl group in position 4 and a halogen in position 5 of the salicyl ring improved the physicochemical properties of compounds bearing two trifluoromethyl groups in the anilide ring while maintaining potency in leukemia cells and KIX-KID interaction inhibition with low toxicity to normal bone marrow cells.

### Acknowledgments

We would like to acknowledge Vivian Zhang, Grace Lam, and Dr. Ludmila Alexandrova for technical assistance. The authors are thankful to Nanosyn, Inc. for supply of specific salicylamides (see **Supplemental Information**). This research was supported by SPARK Pilot Grant Program, Pediatric Cancer Research Foundation, Bear Necessities Foundation, Leukemia & Lymphoma Society Screen to Lead Program, Almalechs and Stanford Translation & Clinical Innovation Award, and Maternal & Child Health Research Institute at Stanford (K.M.S.).

### References

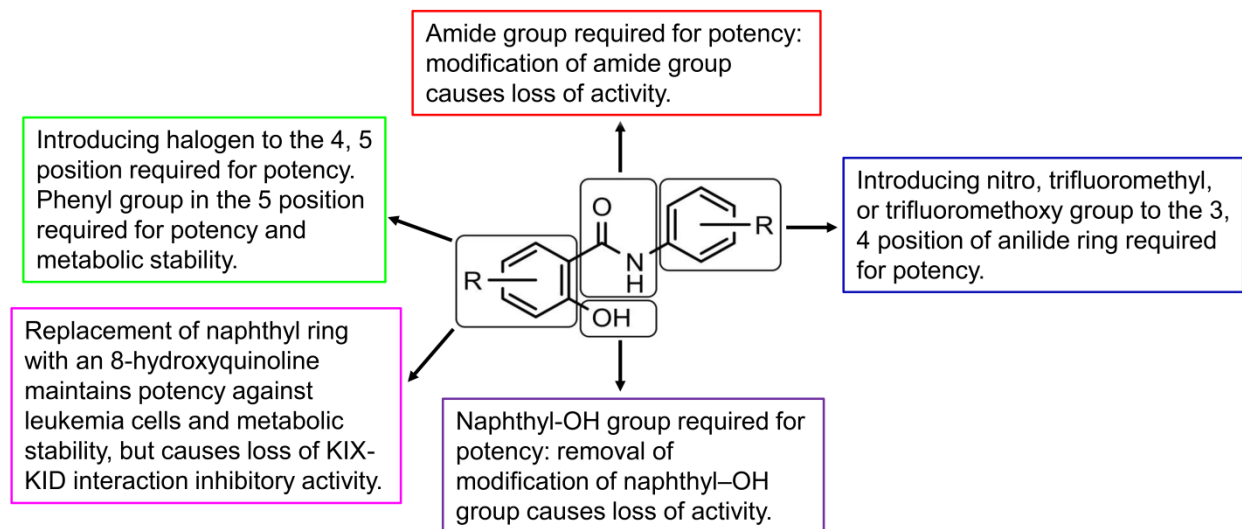
1. Saygin C, Carraway HE. Emerging therapies for acute myeloid leukemia. *J Hematol Oncol.* 2017;10(1): 93.
2. Phelan KW, Advani AS. Novel Therapies in Acute Lymphoblastic Leukemia. *Curr Hematol Malig Rep.* 2018;13(4): 289-299.

3. Dores GM, Devesa SS, Curtis RE, Linet MS, Morton LM. Acute leukemia incidence and patient survival among children and adults in the United States, 2001-2007. *Blood*. 2012;119(1): 34-43.
4. Siegel RL, Miller KD, Jemal A. Cancer statistics, 2018. *CA Cancer J Clin*. 2018;68(1): 7-30.
5. Noone AM, Hanley H, Krapcho M, Miller D, Brest A, Yu M, Ruhl J, Tatalovich Z, Mariotto A, Lewis DR, Chen HS, Feuer EJ, Cronin KA (eds). SEER Cancer Statistics Review, 1975-2015. National Cancer Institute; 2018.
6. Kanellopoulos A, Hamre HM, Dahl AA, Fossa SD, Ruud E. Factors associated with poor quality of life in survivors of childhood acute lymphoblastic leukemia and lymphoma. *Pediatr Blood Cancer*. 2013;60(5): 849-855.
7. Oeffinger KC, Hudson MM. Long-term complications following childhood and adolescent cancer: foundations for providing risk-based health care for survivors. *CA Cancer J Clin*. 2004;54(4): 208-236.
8. Schultz KA, Chen L, Chen Z, et al. Health conditions and quality of life in survivors of childhood acute myeloid leukemia comparing post remission chemotherapy to BMT: a report from the children's oncology group. *Pediatr Blood Cancer*. 2014;61(4): 729-736.
9. Takei H, Kobayashi SS. Targeting transcription factors in acute myeloid leukemia. *Int J Hematol*. 2019;109(1): 28-34.
10. Illendula A, Pulikkan JA, Zong H, et al. Chemical biology. A small-molecule inhibitor of the aberrant transcription factor CBFbeta-SMMHC delays leukemia in mice. *Science*. 2015;347(6223): 779-784.
11. Uttarkar S, Dukare S, Bopp B, Goblirsch M, Jose J, Klempnauer KH. Naphthol AS-E Phosphate Inhibits the Activity of the Transcription Factor Myb by Blocking the Interaction with the KIX Domain of the Coactivator p300. *Mol Cancer Ther*. 2015;14(6): 1276-1285.
12. Shankar DB, Cheng JC, Kinjo K, et al. The role of CREB as a proto-oncogene in hematopoiesis and in acute myeloid leukemia. *Cancer cell*. 2005;7(4): 351-362.

13. Kornblau S, Wu WH, Qiu YH, et al. CREB/ATF Family Protein Expression States in AML: Active CREB1, but not ATF is an Adverse Prognostic Factor. *American Society of Hematology Annual Meeting*. San Francisco, CA.; 2014:Abstract #2344.
14. Cheng JC, Kinjo K, Judelson DR, et al. CREB is a critical regulator of normal hematopoiesis and leukemogenesis. *Blood*. 2008;111(3): 1182-1192.
15. Pellegrini M, Cheng JC, Voutila J, et al. Expression profile of CREB knockdown in myeloid leukemia cells. *BMC cancer*. 2008;8: 264.
16. Chrivia JC, Kwok RP, Lamb N, Hagiwara M, Montminy MR, Goodman RH. Phosphorylated CREB binds specifically to the nuclear protein CBP. *Nature*. 1993;365(6449): 855-859.
17. Kwok RP, Lundblad JR, Chrivia JC, et al. Nuclear protein CBP is a coactivator for the transcription factor CREB. *Nature*. 1994;370(6486): 223-226.
18. Haus-Seuffert P, Meisterernst M. Mechanisms of transcriptional activation of cAMP-responsive element-binding protein CREB. *Mol Cell Biochem*. 2000;212(1-2): 5-9.
19. Best JL, Amezcua CA, Mayr B, et al. Identification of small-molecule antagonists that inhibit an activator: coactivator interaction. *Proceedings of the National Academy of Sciences of the United States of America*. 2004;101(51): 17622-17627.
20. Li BX, Xiao X. Discovery of a small-molecule inhibitor of the KIX-KID interaction. *Chembiochem : a European journal of chemical biology*. 2009;10(17): 2721-2724.
21. Li BX, Yamanaka K, Xiao X. Structure-activity relationship studies of naphthol AS-E and its derivatives as anticancer agents by inhibiting CREB-mediated gene transcription. *Bioorg Med Chem*. 2012;20(23): 6811-6820.
22. Mitton B, Chae HD, Hsu K, et al. Small molecule inhibition of cAMP response element binding protein in human acute myeloid leukemia cells. *Leukemia*. 2016;30(12): 2302-2311.
23. Andrews P, Thyssen J, Lorke D. The biology and toxicology of molluscicides, Bayluscide. *Pharmacol Ther*. 1982;19(2): 245-295.

24. Pearson RD, Hewlett EL. Niclosamide therapy for tapeworm infections. *Ann Intern Med.* 1985;102(4): 550-551.
25. Chen W, Mook RA, Jr., Premont RT, Wang J. Niclosamide: Beyond an antihelminthic drug. *Cell Signal.* 2017.
26. Li Y, Li PK, Roberts MJ, Arend RC, Samant RS, Buchsbaum DJ. Multi-targeted therapy of cancer by niclosamide: A new application for an old drug. *Cancer Lett.* 2014;349(1): 8-14.
27. Moskaleva EY, Perevozchikova VG, Zhirnik AS, Severin SE. [Molecular mechanisms of niclosamide antitumor activity]. *Biomed Khim.* 2015;61(6): 680-693.
28. Jin Y, Lu Z, Ding K, et al. Antineoplastic mechanisms of niclosamide in acute myelogenous leukemia stem cells: inactivation of the NF-kappaB pathway and generation of reactive oxygen species. *Cancer Res.* 2010;70(6): 2516-2527.
29. Ren X, Duan L, He Q, et al. Identification of Niclosamide as a New Small-Molecule Inhibitor of the STAT3 Signaling Pathway. *ACS Med Chem Lett.* 2010;1(9): 454-459.
30. Fonseca BD, Diering GH, Bidinosti MA, et al. Structure-activity analysis of niclosamide reveals potential role for cytoplasmic pH in control of mammalian target of rapamycin complex 1 (mTORC1) signaling. *J Biol Chem.* 2012;287(21): 17530-17545.
31. Chae HD, Cox N, Dahl GV, et al. Niclosamide suppresses acute myeloid leukemia cell proliferation through inhibition of CREB-dependent signaling pathways. *Oncotarget.* 2018;9(4): 4301-4317.
32. Al-Hadiya BM. Niclosamide: comprehensive profile. *Profiles Drug Subst Excip Relat Methodol.* 2005;32: 67-96.
33. Singh JK SA, Shirsath VS. Comparative in-vitro Intrinsic Clearance of Imipramine in Multiple Species Liver Microsomes: Human, Rat, Mouse and Dog. *J Drug Metab Toxicol.* 2012;3(4): 126.
34. Lazebnik YA, Kaufmann SH, Desnoyers S, Poirier GG, Earnshaw WC. Cleavage of poly(ADP-ribose) polymerase by a proteinase with properties like ICE. *Nature.* 1994;371(6495): 346-347.

35. Nicolas E, Golemis EA, Arora S. POLD1: Central mediator of DNA replication and repair, and implication in cancer and other pathologies. *Gene*. 2016;590(1): 128-141.
36. Chae HD, Mitton B, Lacayo NJ, Sakamoto KM. Replication factor C3 is a CREB target gene that regulates cell cycle progression through the modulation of chromatin loading of PCNA. *Leukemia*. 2015;29(6): 1379-1389.
37. Mitton B, Hsu K, Dutta R, et al. Small molecule screen for inhibitors of expression from canonical CREB response element-containing promoters. *Oncotarget*. 2016;7(8): 8653-8662.



ACCEPTED MANUSCRIPT